

Selective Complexation of UO_2^{2+} by the Calix[6]arene $^{6-}$ Anion: Structure and Hydration Studied by Molecular Dynamics Simulations

P. GUILBAUD and G. WIPFF*

URA 422 CNRS, Institut de Chimie, 4, rue B. Pascal, 67000 Strasbourg, France.

(Received: 29 July 1993; in final form: 15 October 1993)

Abstract. Based on molecular dynamics simulations, we describe the structure and solvation pattern of the *p*-Me-calix[6]arene $^{6-}$ anion in the free state, and complexed with UO_2^{2+} in aqueous solution. UO_2^{2+} is coordinated in its equatorial plane to five phenolate oxygens, and has no direct coordination with water molecules. The closest water molecules are strongly hydrogen bonded to the ligand. The complex of the *p*-Me-calix[5]arene $^{5-}$ anion with UO_2^{2+} displays similar binding and solvation features. For the purpose of comparison, a complex of *p*-Me-calix[6]arene $^{6-}$ with a spherical divalent cation, referred to as 'Cu $^{2+}$ ' is simulated under the same conditions. In the most stable conformer, Cu $^{2+}$ is coordinated to four phenolic oxygens in a square planar arrangement, and to one water molecule. An energy component analysis suggests that the high binding selectivity of the calixarene for uranyl relates to a large cation-guest interaction, and to a better hydration of the complex. In the UO_2^{2+} complex the strong hydration of the negatively charged ligand is not significantly prevented by the complexed cation, unlike in the spherical cation complexes. It is stressed that entropic effects, which are not amenable to such calculations, play an important role in the binding selectivity of these calix[6] and calix[5]arenes for uranyl.

Key words: Calixarene, uranyl, solvation, molecular dynamics, molecular recognition, ionophore.

1. Introduction

Selective extraction of uranyl from sea water or from nuclear wastes, based on selective binding by synthetic ionophores, is very important in the context of energy resources [1]. The *p*-sulfonato calix[*n*]arenes (*n* = 4, 5, 6) [2–5] (Figure 1) present a particularly interesting class of ionophores, since calixarenes can be easily synthesized [6, 7], and the calix[5] and calix[6] derivatives complex UO_2^{2+} very efficiently [3] ($\log K$ is 18.9 and 19.2, respectively, at pH = 10.5). For the calix[4] derivative, the binding drops markedly ($\log K = 3.2$ at pH 6.5). The binding selectivity of calix[6]arene for UO_2^{2+} , compared to other divalent cations such as Ni $^{2+}$, Zn $^{2+}$ and Cu $^{2+}$, is high ($K_{\text{uranyl}}/K_{\text{M}^{2+}}$ is $10^{17.0}$, $10^{13.7}$ and $10^{10.6}$, respectively). However, the structural and thermodynamic basis of these binding features and selectivity, although very important in designing new uranophiles, remain poorly understood.

* Author for correspondence.

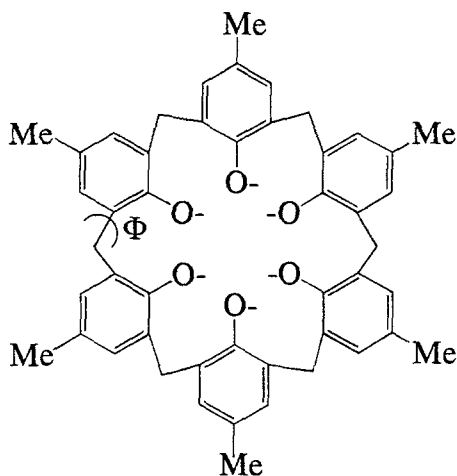
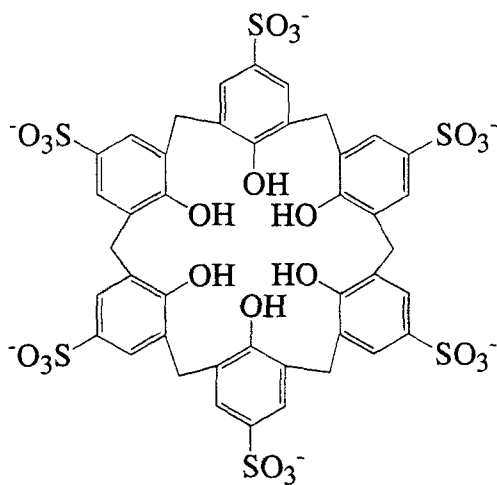


Fig. 1. Structure of *p*-sulfonato calix[6]arene (top) and *p*-Me-calix[6]arene⁶⁻ **Calix6** (bottom).

Solid state structures, although possibly irrelevant to the picturing of structures in solution, remain essential in establishing the nature of the complex, and providing a basis for analyzing the interplay between host-guest interactions and conformations of these partners [8]. In contrast to the alkali and alkaline earth cation complexes with macrocyclic receptors, for which many structural and thermodynamic data are available [9, 10] relatively few are available for uranyl complexes with ionophores [11, 12]. In X-ray structures of UO_2^{2+} complexes with neutral macrocyclic ligands, such as crown ethers, either inclusive or noninclusive coordination of the cation can be observed [13–15]. However, no X-ray structure of the UO_2^{2+} complexes of calix[5] and calix[6]arenes is available. Following the concept of first shell ‘solvation’ of the cation by the binding sites of the ligand [10, 16, 17],

we investigated the hydration of UO_2^{2+} , and of its NO_3^- and 18-crown-6 adducts, as a first theoretical approach to the design of uranophiles [18].

In the solid state structures, UO_2^{2+} is bound in the equatorial plane by five or six heteroatoms [1, 13, 14, 19–31] and it is reasonable to assume that calix[5]arene and calix[6]arene also bind UO_2^{2+} with their phenolic oxygens, as observed for ligands such as CO_3^{2-} , CH_3COO^- , NO_3^- , H_2O , etc., and other ligands containing heteroatoms, such as crown ethers. Two solid state structures are available for the free calix[6]arene. The water soluble *p*-sulfonato derivative has been shown [4], to adopt a ‘double partial cone’ conformation. In contrast, the water insoluble *p*-*t*-butyl derivative displays an ‘ellipsoidal cone’ [32]. Neither of these structures looks optimal for binding UO_2^{2+} without conformational changes, in order to achieve equatorial coordination to the U atom. As shown for typical ionophores such as 18-crown-6 or the 222 cryptand, the conformational state of the free calixarene may not be representative of the complexed states. Solvent and environment effects may also play an important role in preferred conformations and binding selectivities [33].

The aim of this study is to simulate the calix[6]arene in its free state and complexed by UO_2^{2+} , in the gas phase and in aqueous solution, in order to characterize its conformation and the binding mode to the cation. The question of structure, solvation, and binding selectivity for UO_2^{2+} in comparison with other divalent spherical cations, is also investigated by molecular dynamics (MD) simulations using an explicit representation of the solvent. The complex of UO_2^{2+} with *p*-Me-calix[5]arene is also investigated in water.

Computer simulation methods allow one to investigate ionophores and ions in solution [33–41] and give microscopic views of solvation features. Host-guest chemistry is a particularly rich field for such studies, given the amount of experimental data available for comparison, and the relatively small size of the ‘super-molecules’ [35]. In the field of calixarenes, computational work has been performed using MM2 molecular mechanisms calculations on calix[4]arene by Royer *et al.* [42], who investigated the question of the cone’s conformation and inter-conversions. Miyamoto and Kollman [43] performed MD simulations and free energy calculations on calix-spherands and their complexes with Na^+ , K^+ and Rb^+ . Grootenhuis *et al.* investigated structural, energetic and acid/base properties of *p*-methylcalix[4]arenes [44]. Recently, extensive MD simulations in water and in acetonitrile on calix[4]arenes, functionalized at the lower rim, addressed the question of (pre)organization and ligand wrapping around the cation as a function of the solvent and of the cationic guest [45, 46]. In particular, it was shown that the coordination pattern and conformation observed in the X-ray structure of the K^+ complex does not correspond to those in water or acetonitrile solutions. The binding selectivity for Li^+ in acetonitrile was also correctly predicted using free energy simulations. In the following, we investigate how the calix[6]arene binds UO_2^{2+} in water, with specific features compared to a spherical cation, which will be referred to henceforth as Cu^{2+} .

2. Methods

All calculations were performed with the AMBER4.0 [47, 48] software, using the following representation of the potential energy:

$$\begin{aligned}
 E_{\text{pot}} = & \sum_{\text{bonds}} K_b (r - r_{\text{eq}})^2 + \sum_{\text{angles}} K_\theta (\theta - \theta_{\text{eq}})^2 \\
 & + \sum_{\text{dihedrals}} V_n \left(1 + \cos(n\varphi - \gamma) \right) \\
 & + \sum_{i < j} \left(\varepsilon_{ij} \left((R^*/R_{ij})^{12} - (R^*/R_{ij})^6 \right) + q_i q_j / \varepsilon R_{ij} \right) \\
 & + \sum_{\text{H-bonds}} \varepsilon_{ij} \left((R^*/R_{ij})^{12} - (R^*/R_{ij})^{10} \right).
 \end{aligned}$$

The deformation of bonds, angles and dihedrals are described in the harmonic approximation. The van der Waals and Coulombic interactions are calculated for all atoms separated by at least three bonds. The atomic charges and force field parameters on the calixarene anionic unit have been taken from the work of Grootenhuis *et al.* [45]. The only difference concerns the choice of force constants on improper dihedrals which have been increased to 292 kJ mol⁻¹ in order to ensure near planarity of the aromatic moieties at high temperature MD. The AMBER 1-10-12 potential has been used for hydrogen bonds between the solvent and the solute (phenolates oxygens and O_{uranyl}). Water has been described in the TIP3P model ($q_o = -0.834$; $q_H = 0.417$) [17]. A 10 Å cut-off truncation for non-bonded interactions involving the solvent is used. Uranyl parameters are those used in a previous study [18] ($q_u = +4$, $R_{u^*} = 1.6$ Å and $\varepsilon_u = 0.5$ kJ mol⁻¹; $q_o = -1$, $R_{o^*} = 1.6$ Å and $\varepsilon_o = 0.63$ kJ mol⁻¹). The spherical divalent cation which is simply represented with its van der Waals radius ($R^* = 1.2$ Å) and its charge (+2) will be referred to as Cu²⁺. In this model the 'bonds' between the ligand and Cu²⁺ are therefore represented as purely noncovalent, and result from the electrostatic attraction between the cation and the negatively charged binding sites, which therefore have no directionality. In comparison with a covalent model, this representation allows ligand exchanges and reorientation along the MD simulation.

2.1. CHOICE OF STARTING STRUCTURES

Our model assumes that coordination of the cations involves the phenolate oxygens only, and the calix[6]arene was simulated as the *p*-Me instead of the *p*-sulfonato derivatives, for simplicity. Although the remote sulfonates may increase the electrostatic ion binding by the phenolate oxygens [49], they are not likely to contribute significantly to the selectivity for uranyl, compared to spherical ions. From a com-

putational point of view, explicit representation of the sulfonates without neutralizing counterions may be questionable, based on computer experience gained in the field of nucleic acids. Modeling the sulfonato derivative would cause additional problems related to the treatment of electrostatic effects with a highly charged receptor. In the case of alkali cation complexes of calix[4]arenetetraamide, we computationally compared *p*-sulfonato with *p*-*t*-butyl derivatives in water, and found that the structure and binding properties at the lower rim were not significantly modified by remote solubilizing groups [50]. After 50–100 ps of MD simulations, the position of the cation and its coordination pattern to the amidic carbonyls were found to be similar in both derivatives.

Since force field and MD simulations cannot picture bond making or breaking processes involved in proton transfers, we selected all of the phenolic oxygens in their unprotonated state, in order to provide optimal binding capabilities to the complexed cation. This is indeed a reasonable hypothesis based on the pH dependence of the binding studied by Shinkai *et al.* [3, 5] and others [7]. In the following, this *p*-Me-calix[6]arene⁶⁻ anion will be referred to as **Calix6** (Figure 1). The starting structure of **Calix6** and its complexes is modelled with the flattened cone $+-,+-,+-,+-,+-,+-$ conformation of C_{6v} symmetry (Figure 2). A similar cone conformation is also used as a starting model of the *p*-Me-calix[5]arene UO_2^{2+} complex in water ($+-,+-,+-,+-,+-$).

We first studied the free ligand **Calix6** and its Cu^{2+} and UO_2^{2+} complexes in the gas phase, in order to use MD to sample their structures for 100 ps at high temperature (1000 K). The most stable form obtained in the gas phase was then immersed in a bath of water molecules, and MD simulations were performed for at least 50 ps (Table I). In fact, because of the strong cation – oxygen attractions, only a limited number of structures appeared, which will be briefly described. For the UO_2^{2+} and Cu^{2+} complexes, two different conformations were characterized. In order to ensure that they are determined by the cationic guest rather than from artefacts, we permuted the two cations from these two conformers, and reran at least 50 ps of MD in water (Table I).

2.2. ANALYSIS OF RESULTS

Because of the large size and flexibility of calix[6]arene, its conformational state cannot be as easily defined as for the smaller analogues. We therefore used the symbolic representation defined by Uguzzoli and Andreetti [51], based on the values of the C-C-CH₂-C dihedral Φ angles (Figure 1). The ‘double partial cone’ of *p*-sulfonato-calix[6]arene is defined by $+-,+-,+,+-,+-,--$ and the *p*-*t*-butyl-calix[6]arene by $+-,+-,+,+-,+-,+-$. We also use the ‘up’ and ‘down’ terminology to characterize schematically the orientation of each phenolate group, which is either in the cone direction, or ‘inverted’. Structural and energy analysis was performed with our MD-DRAW and MDS software [52] from the trajectories, which were saved every 0.2 ps; time averages are reported in the tables, togeth-

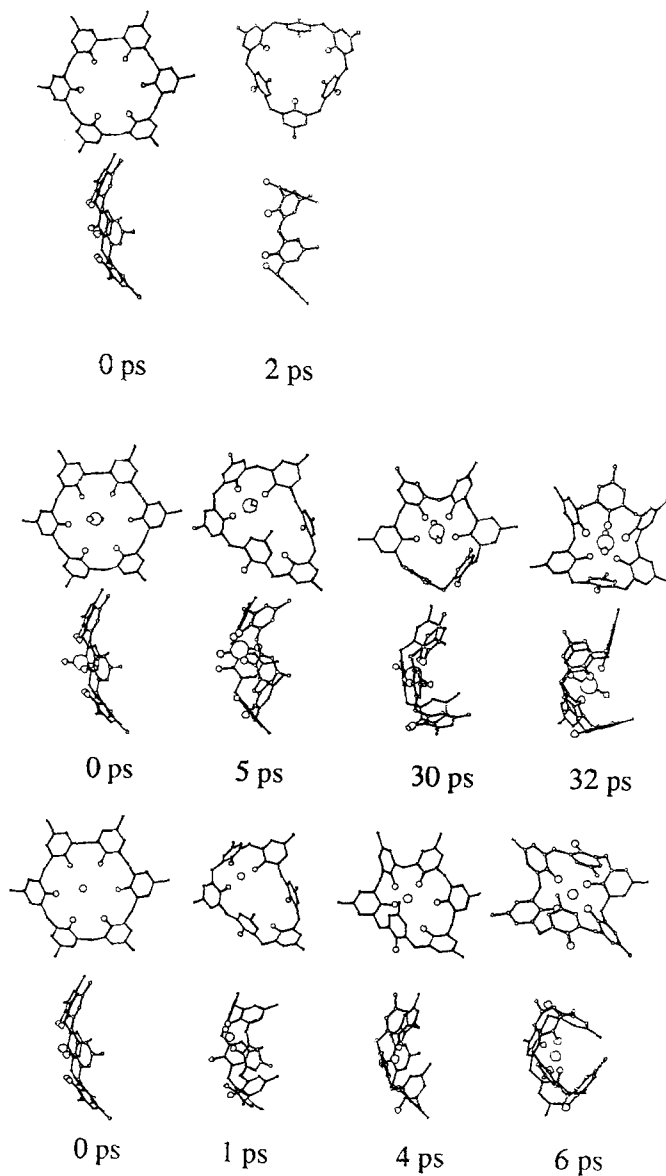


Fig. 2. Structures obtained during the 'simulated quenching' of the free **Calix6** (top), the **Calix6-UO₂²⁺** complex (middle), and the **Calix6-Cu²⁺** complex (bottom). Orthogonal views.

er with the statistical fluctuations. The solute-solvent interaction energy will be referred to as 'solvation energy' for short, since it is the dominant component of the enthalpy of solvation.

TABLE I. MD simulations in water, simulation times and water box characterization.

System		Simulation time (ps)	Water box size (Å)	Number of water molecules
Free calix[6]arene ⁶⁻		70	36.3*36.3*30.6	1043
Calix[6]arene ⁶⁻ UO ₂ ²⁺	a	100	36.9*35.4*28.7	1126
	b	50	38.0*35.4*28.7	1103
Calix[6]arene ⁶⁻ Cu ²⁺	a	50	37.0*32.1*30.1	1023
	b	50	36.2*35.9*31.5	1152

^a The starting structure is obtained from the gas phase simulation.

^b The starting conformation of the ligand is, for UO₂²⁺, the one obtained in the gas phase for the Cu²⁺ complex; and for Cu²⁺, the one obtained in the gas phase for the UO₂²⁺ complex.

3. Results

3.1. THE CALIX6-UO₂²⁺ AND CALIX6-CU²⁺ COMPLEXES IN THE GAS PHASE. NON-PLANARITY OF THE LIGAND

Calix6 and its Cu²⁺ and UO₂²⁺ complexes are first modeled in the gas phase in order to compare their low-energy structures. This is achieved by the ‘simulated quenching’, consisting of a single MD simulation at high temperature (1000 K) from which structures are regularly extracted and energy minimized ($T = 0$ K). The high kinetic energy at 1000 K in principle allows sampling regions of conformational space separated by high energy barriers.

For each system, ‘simulated quenching’ has been performed from a 100 ps MD simulation with one structure minimized every picosecond, thus generating 100 minimized structures. We find that the number of interconversions and structures produced is low, despite the high temperature used, in contrast to what was observed with the 222 cryptands [33]. Figure 2 shows that the lowest energy structures are obtained at 32 ps and 6 ps, respectively, for the UO₂²⁺ and the Cu²⁺ complexes, and at 2 ps for the free **Calix6**. The free **Calix6** roughly retains the ‘cone’ conformation (+-,+-,+-,+-,+-,+-), deformed by repulsions between the phenolic oxygens. In the UO₂²⁺ complex the U atom is coordinated to five phenolic oxygens (Figure 2 and Table II), and the calixarene has an alternate cone conformation with one phenol ‘up’ and five ‘down’ (+-,+-,+-,+-,+,-,+). In the Cu²⁺ complex the cation is coordinated to four phenolic oxygens only (Table II), and the ligand adopts another conformation (+-,+,-,-,+,-,+,-,-), such that two phenols are ‘up’ and four ‘down’.

TABLE II. Metal...O_p average distances within the UO₂²⁺ and Cu²⁺ complexes of the **Calix6** (distances are given in Å; all fluctuations are about 0.1 Å).

	O ₁	O ₂	O ₃	O ₄	O ₅	O ₆
Cu ²⁺ gas	1.95	4.83	1.91	1.95	4.61	1.86
Cu ²⁺ /1 water	1.90	4.61	1.89	1.90	4.55	1.89
Cu ²⁺ /2 water	1.90	1.91	4.6	1.91	1.91	3.44
UO ₂ ²⁺ gas	2.18	2.04	4.78	2.06	2.08	2.05
UO ₂ ²⁺ water	2.16	2.17	4.8	2.18	2.16	2.18

Analysis of the time evolution of some energy components for the minimized structures of the **Calix6**-UO₂²⁺ complex shows that an energy barrier is passed after 30 ps of MD, leading to a stabilization of the complex of 585 kJ mol⁻¹. It corresponds to a change in the cation coordination and in the conformation of the calixarene (Figure 2). The calixarene itself is destabilized by 1045 kJ mol⁻¹, but the concomitant increase of the cation/cage attraction (1670 kJ mol⁻¹) largely compensates for that.

There are therefore good reasons to believe that the only structure produced by the 'simulated quenching' is very stable, and that this is a feature of the system, rather than a result of being trapped in a single conformation. Indeed, using the same procedure for the free calix[6]arene in its neutral state, led to a structure which is quasi-identical to Atwood's structure [4], which became available to us later, and to the lowest energy structure modeled by Groenen [53].

3.2. CALIX6 IN FREE STATE AND COMPLEXED BY UO₂²⁺ AND Cu²⁺ IN WATER

3.2.1. Free Calix[6]arene⁶⁻

Figure 3 displays a snapshot of the free **Calix6** in water after 30 ps of MD simulation, including all water molecules within 3 Å of each phenolic oxygen. In water, the calixarene retains its 'cone' conformation, as in the gas phase (+-,+-,+-,+-,+-,+ -), with small deformations, related to solvation effects. In fact, water molecules enter into the 'cone' to form strong hydrogen bonds with some phenolic oxygens (Figure 3).

Table III gives the characteristics of the water RDFs (radial distribution functions) around each phenolic oxygen (O_p). Figure 4 represents the average of these RDFs. Each phenolic oxygen is solvated by about four water molecules, where the proton lies at 1.9 Å.

Energy component analysis (Table IV) shows that the average interaction energy between **Calix6** and these first water molecules is highly attractive (-1790 kJ mol⁻¹), and represents about 1/3 of the **Calix6** solvation energy. The internal

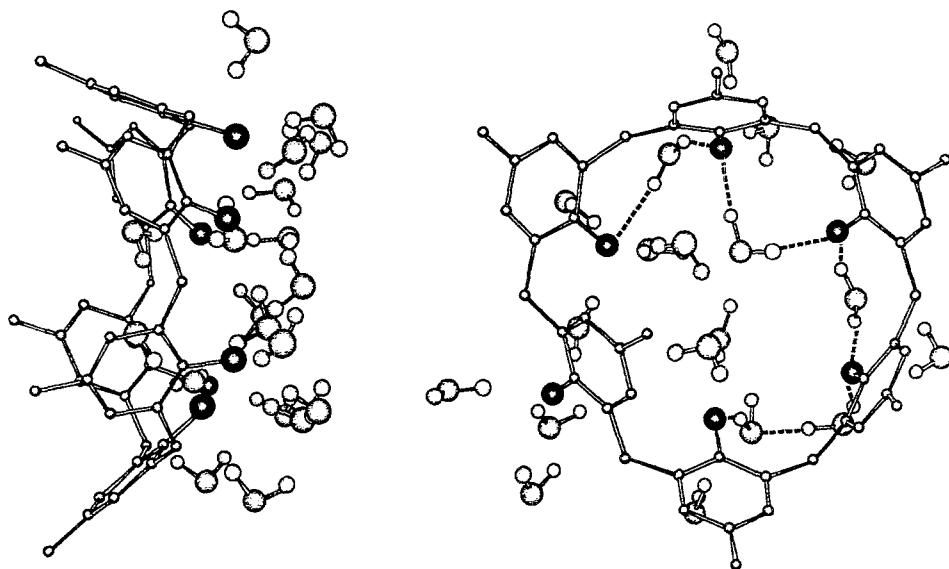


Fig. 3. The free **Calix6** in water including water molecules within 3 Å from each phenolic oxygen. Snapshot after 70 ps of MD. Orthogonal views.

TABLE III. Free **Calix6** in water: RDF characteristics.

Center	1st peak for H _w		1st peak for O _w	
	position (Å)	<i>N</i> H _w ^a	position (Å)	<i>N</i> O _w ^a
O1	1.9	3.8	2.8	4.10
O2	1.9	3.7	2.8	3.94
O3	1.9	3.8	2.8	3.89
O4	1.9	3.7	2.8	3.74
O5	1.9	3.8	2.8	4.05
O6	1.9	3.7	2.8	3.76

^a *N* H_w and *N* O_w correspond to the number of water protons or oxygens, after integration of the first RDF peak.

energy of the free **Calix6** is high (3823 kJ mol⁻¹) due to the important electrostatic strain induced by the six negative charges, which repel each other.

3.2.2. UO_2^{2+} -**Calix[6]arene**⁶⁻ Complex in Water

Two starting geometries were simulated for this complex in water. The first one (+-,+-,+-,+-,+-,+-) comes from the most stable UO_2^{2+} complex obtained *in vacuo*. The second is obtained from the most stable Cu^{2+} complex *in vacuo*

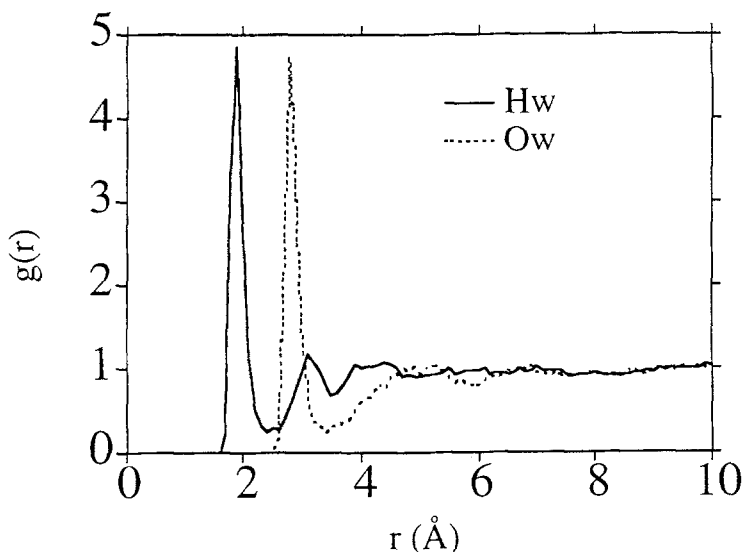


Fig. 4. The free **Calix6** in water. Average of the water RDFs for the six phenolate oxygens.

TABLE IV. Free **Calix6** in water. Energy component analysis based on the interaction of 3 groups: the calixarene, water molecules at less than 3 Å of each phenolic oxygen, and the other water molecules. Average energies and statistical fluctuations, from the MD trajectories, in kJ mol^{-1} .

	Calix6	First oxygens water shell	Other water molecules
Calix 6	3823 ± 10	-1794 ± 16	-3413 ± 23
first oxygens water shell		275 ± 5	-614 ± 10
Other water molecules			-31718 ± 142

(+-,+-,--,+-,+-,--) in which Cu^{2+} is replaced by UO_2^{2+} . In water both simulations lead to the same conformation of the complex. Indeed, the second UO_2^{2+} complex became identical to the first one in less than two picoseconds. We therefore present only the results of the first MD simulation (Figure 2).

Figure 5 shows the UO_2^{2+} -**Calix6** complex in water after 100 ps of MD, with all water molecules within 5 Å of the U atom. The conformation is not very different from the one obtained *in vacuo* (+-,+-,+-,+-,-+,-+). The UO_2^{2+} cation is

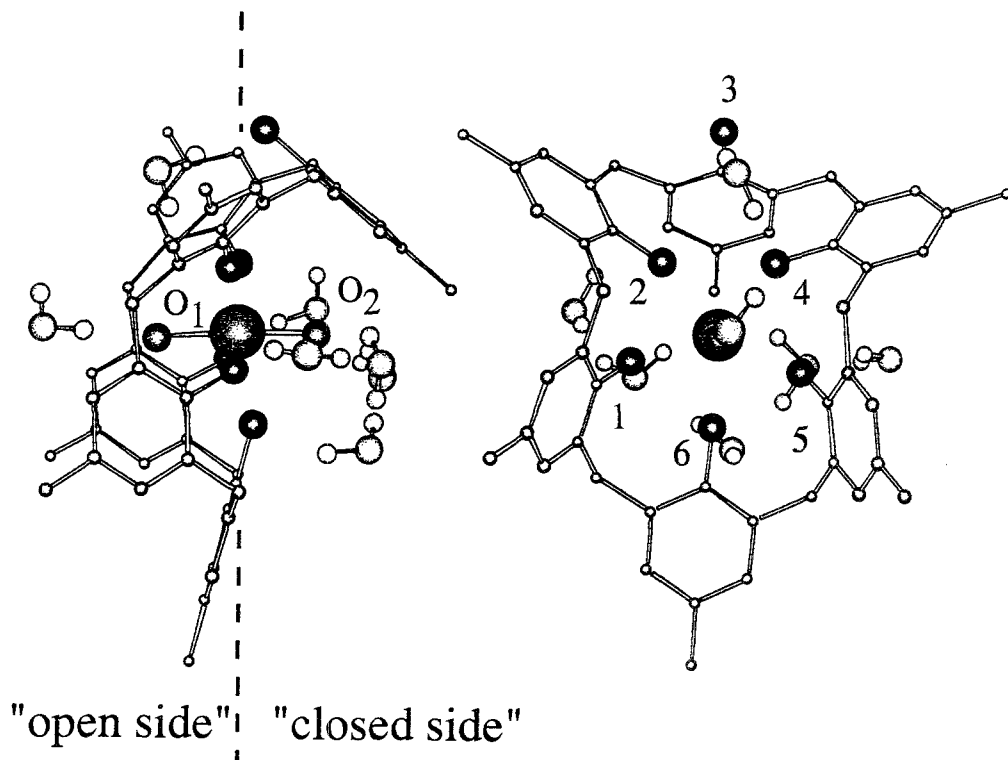


Fig. 5. The **Calix6**- UO_2^{2+} complex in water with the water molecules within 5 Å from the U atom. Snapshot after 100 ps of MD. Orthogonal views.

coordinated to five phenolic oxygens in its equatorial plane, which are at 2.17 Å from the U atom (Table II).

For UO_2^{2+} uncomplexed in water, MD simulations revealed that five H_2O molecules coordinate the U atom in the equatorial plane of the cation, and about two H_2O solvate each O atom [18]. Some of these water molecules have the O-H dipole oriented antiparallel to the O-U dipole of UO_2^{2+} . In the UO_2^{2+} -**Calix6** complex, no water molecule is coordinated to U. The $\text{U}\cdots\text{H}_\text{W}$ RDF presents a peak at 3.5 Å (about 14 water protons), and the $\text{U}\cdots\text{O}_\text{W}$ RDF has a peak at 4.2 Å (about 7 oxygen atoms). These peaks correspond, in fact, to the first solvation shell of the phenolate oxygens and of the uranyl oxygens, rather than of the U atom (Figure 6 and Table V). The corresponding water molecules are oriented with the O-H dipole parallel to the O-U dipole.

The interaction energy analysis based on four groups (UO_2^{2+} , the **Calix6**, the first solvation shell of the complex, and the other water molecules) is consistent with this solvation pattern (Table VI): the UO_2^{2+} /first water shell interaction is repulsive (376 kJ mol^{-1}), whereas the **Calix6**/first water shell interaction is more than twice

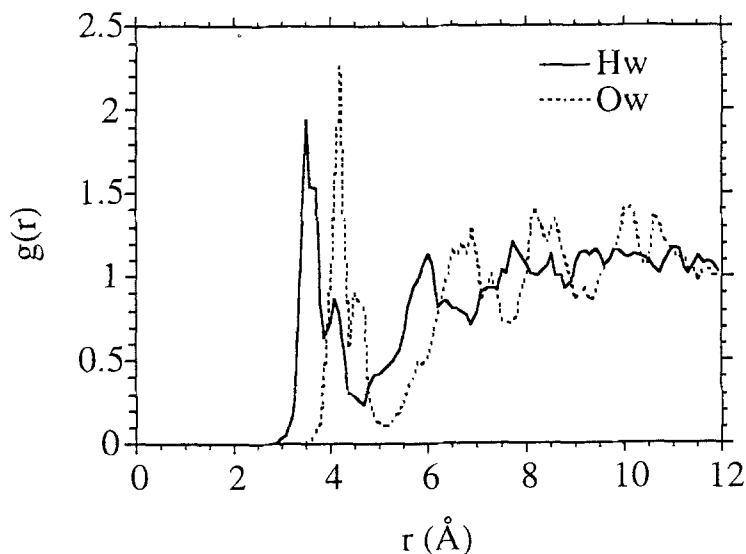


Fig. 6. The Calix6- UO_2^{2+} complex in water, $\text{U}\cdot\text{O}_w$ and $\text{U}\cdot\text{H}_w$ RDFs.

TABLE V. Calix6- UO_2^{2+} in water: RDF characteristics.

Calix6 Center	1st peak for H_w		1st peak for O_w	
	position (Å)	$N \text{H}_w^a$	position (Å)	$N \text{O}_w^a$
O1	1.9	0.9	2.8	1.0
O2	2.9	3.5	3.1	1.7
O3	1.9	3.9	2.8	3.9
O4	2.0	0.8	2.9	1.1
O5	1.9	0.9	2.8	0.9
O6	1.9	0.9	2.9	0.9

Center	1st peak for H_w		2nd peak for H_w		1st peak for O_w	
	position (Å)	$N \text{H}_w^a$	position (Å)	$N \text{O}_w^a$	position (Å)	$N \text{O}_w^a$
U	3.5	13.4	no peak		4.2	7.1
O1	1.8	1.3	3.2	6.2	2.8	1.4
O2	1.9	2.2	2.7	6.2	2.8	2.8

^a $N \text{H}_w$ and $N \text{O}_w$ correspond to the number of water protons or oxygens, after integration of the first RDF peak.

TABLE VI. **Calix6**- UO_2^{2+} in water. Energy component analysis based on the interaction of 4 groups: the calixarene, the UO_2^{2+} ion, the water molecules at less than 5 Å from U, and the other water molecules. Average energies and statistical fluctuations from the MD trajectories, given in kJ mol^{-1} .

	UO_2^{2+}	Calix6	Water shell at 5 Å from U	Other water molecules
UO_2^{2+}	42±4	-6257±2	376±3	838± 4
Calix6		4932±4	-970±6	-3348± 12
Water shell at 5 Å from U			-31±2	-296± 3
Other water molecules				-49270±326

as attractive (-970 kJ mol^{-1}). This contrasts with other cation complexes with neutral macrocycles, where the cation/water interaction energy is attractive [33].

The UO_2^{2+} cation has larger interactions with the ligand in the complexed state ($-6257 \text{ kJ mol}^{-1}$) than with the first water shell molecules in its free state ($-1672 \text{ kJ mol}^{-1}$). This is because **Calix6** provides a much better environment for UO_2^{2+} than water, thanks to the very negative electrostatic shield in the equatorial plane.

Since the **Calix6** is highly deformed, the two uranyl oxygens have different environments. The first one (O_1), in the 'open' side of the calixarene, is partially shielded from the solvent (Figure 5), and hydrogen bonded to one water molecule. The second oxygen (O_2) in the 'closed' side of the molecule, is more accessible to water and is hydrogen bonded to two water molecules.

The interaction of complexed **Calix6** with water, although still very attractive, is somewhat less than for the free **Calix6** ($-4318 \text{ kJ mol}^{-1}$ and $-5204 \text{ kJ mol}^{-1}$, respectively). This is because the encapsulated UO_2^{2+} cation prevents strong hydrogen bonds to the phenolic oxygens of the ligand. Conversely, the ligand prevents direct coordination of water molecules to the cation. It is stressed, therefore, that the large enthalpic stabilisation of the complex, related to the host-guest attraction, will add a favourable entropy component resulting from the desolvation of the partners and of the complex, compared to the complex with a spherical M^{2+} cation (see next section).

For the calix[5]arene- UO_2^{2+} complex, simulated under the same conditions, a flattened cone conformer is obtained after 50 ps. The U atom is coordinated to five phenolate oxygens, which prevent its direct coordination to water molecules (Figure 7).

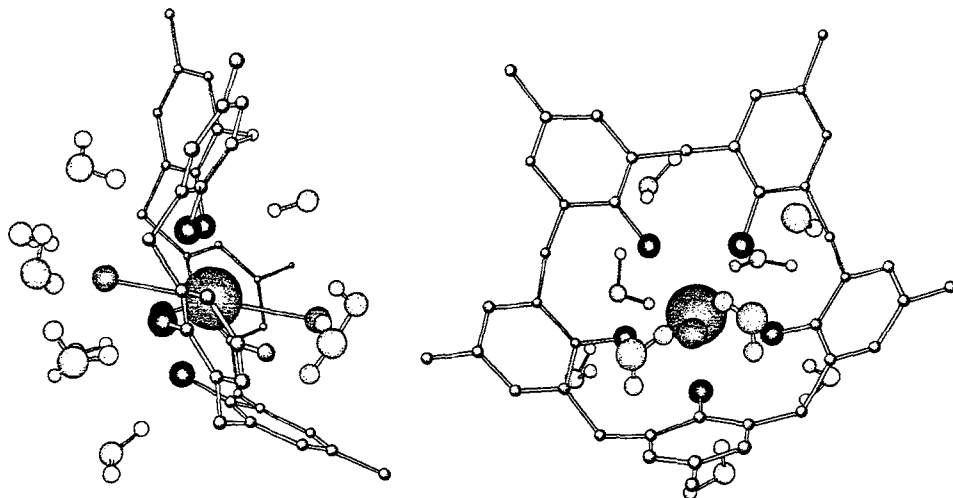


Fig. 7. The *p*-Me-calix[5]arene- UO_2^{2+} complex in water with the water molecules within 5 Å from the U atom. Snapshot after 50 ps of MD. Orthogonal views.

3.2.3. Cu^{2+} -Calix6 Complex in Water

For the simulations on the Cu^{2+} complex in water, two starting conformers of the ligand obtained from the gas phase were used, as for the UO_2^{2+} complex. The first one was obtained from the Cu^{2+} -Calix6 complex in the gas phase, and the second one from the UO_2^{2+} -Calix6 complex, in which UO_2^{2+} was replaced by Cu^{2+} . These two MD simulations in water led to two different structures. The first one remains close to the starting one and is called $\text{Cu}^{2+}/1$ (see Figure 8). The Cu^{2+} cation is still coordinated by four phenolic oxygens at 1.9 Å, and the Calix6 conformation remains $+-,+-,--,+-,+-,--$.

There is no water molecule directly coordinated to Cu^{2+} . The nearest water molecules are coordinated to the phenolic oxygens. The four phenolic oxygens coordinated to Cu^{2+} are solvated by about one water molecule, and the two others by about four water molecules (as in the free Calix6), at less than 1.9 Å. On the 'closed' side of the molecule (Figure 8), the phenyl groups shield the cation from water, and on the 'open' side the phenolate groups provide a negative electrostatic field, which orients the water molecules with their protons pointing to the ligand, giving rise to repulsion with Cu^{2+} .

In the second simulation of the Cu^{2+} complex in water, Cu^{2+} is initially coordinated by five phenolic oxygens (Figure 9). After 10 ps a conformational transition takes place in which one phenolate oxygen bound to Cu^{2+} is replaced by one water molecule ($\text{Cu}^{2+}/2$). The new conformation is $+-,+-,+-,+-,-+,-+$. The cation is then coordinated to four phenolic oxygens (as in $\text{Cu}^{2+}/1$) and one water molecule, which forms a square-based pyramid. Table II gives the average

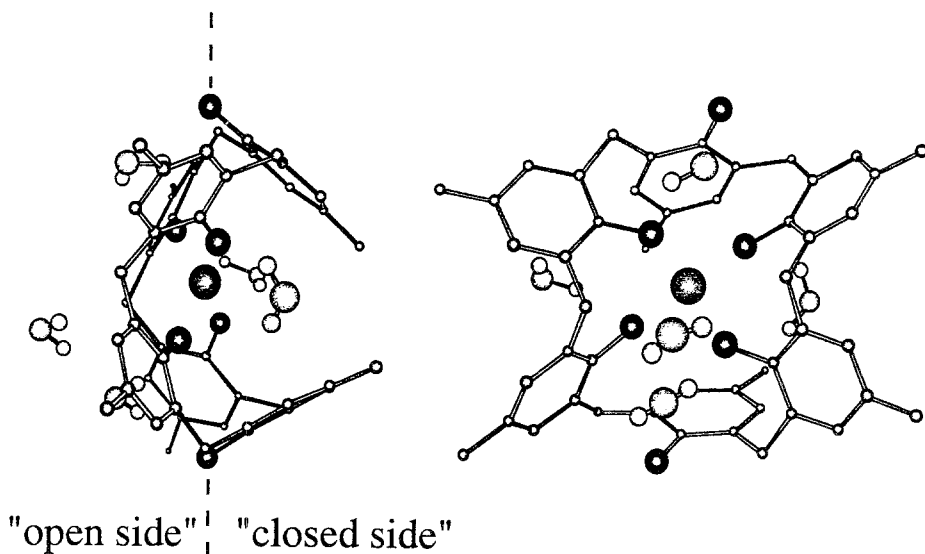


Fig. 8. The $\text{Cu}^{2+}/1$ conformer of the **Calix6**- Cu^{2+} complex in water including the water molecules within 5 Å from Cu^{2+} . Snapshot after 50 ps of MD. Orthogonal views.

$\text{Cu}^{2+}\dots\text{O}_p$ distances along the MD simulation plotted on Figure 10. The cation's accessibility to water is larger than in the $\text{Cu}^{2+}/1$ conformation, where two phenyls are 'down'.

The energy analysis (Table VII) shows that in both $\text{Cu}^{2+}/1$ and $\text{Cu}^{2+}/2$ structures, the $\text{Cu}^{2+}/\text{Calix6}$ attraction energy is similar (about $-5580 \text{ kJ mol}^{-1}$). The other components favour $\text{Cu}^{2+}/2$ over $\text{Cu}^{2+}/1$: the energy of **Calix6** within the complex ($\Delta E = 105 \text{ kJ mol}^{-1}$), and the solvation energy of the complex ($\Delta E = 490 \text{ kJ mol}^{-1}$) with a contribution of 117 kJ mol^{-1} due to the 'first shell' water molecules. It is therefore suggested that the most stable conformer in water is $\text{Cu}^{2+}/2$.

3.2.3.1. Energy Comparison of the UO_2^{2+} and Cu^{2+} Complexes MD simulations do not allow direct comparison of the stability of the complexes. Free energy simulations should be performed for this purpose [58]. However, energy component analysis reveals interesting differences in energy features concerning the complexes and their solvation. The $\text{UO}_2^{2+}/\text{Calix6}$ interaction ($-6257 \text{ kJ mol}^{-1}$) is 670 kJ mol^{-1} better than the $\text{Cu}^{2+}/\text{Calix6}$ interaction energy. The internal energy of **Calix6** is similar within the complexes, as for free **Calix6**. The total solvation energy of the complexes is similar for UO_2^{2+} ($-3106 \text{ kJ mol}^{-1}$) and $\text{Cu}^{2+}/1$ ($-3160 \text{ kJ mol}^{-1}$), and is slightly better for $\text{Cu}^{2+}/2$ ($-3650 \text{ kJ mol}^{-1}$). Another solvation feature favours the UO_2^{2+} over the Cu^{2+} complex. The interaction energy within the first shell water molecules (within 5 Å from UO_2^{2+} and 4.5 Å from Cu^{2+} ,

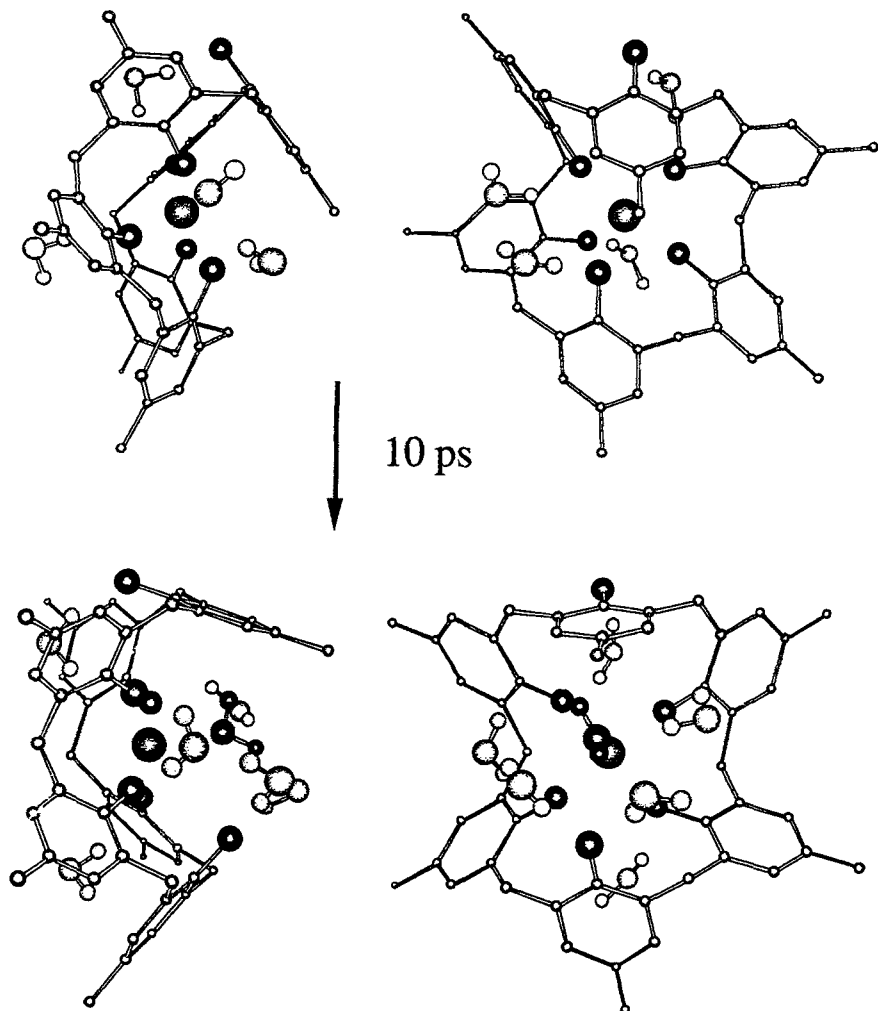


Fig. 9. The $\text{Cu}^{2+}/2$ conformer of the Calix6- Cu^{2+} in water with the water molecules within 3 Å from Cu^{2+} . Snapshots at 1 ps and at 10 ps of MD (see text).

respectively) is slightly attractive for the UO_2^{2+} complex (-30 kJ mol^{-1}), but repulsive for the Cu^{2+} complex (77 kJ mol^{-1}). Although it is not possible to provide a simple explanation of the large $\text{UO}_2^{2+}/\text{Cu}^{2+}$ selectivity, based on the calculations, it is stressed that in addition to the ligand/ionophore interaction, solvation effects play an important role. Analysis of thermodynamic data on macrocyclic complexes involving highly charged substrates and/or receptors does indeed indicate that complexation in water is of entropic, rather than of enthalpic origin [55–57]. It would be desirable to perform such measurements for these calixarene complexes. We suggest that the entropic contributions favour UO_2^{2+} over spherical cations, since

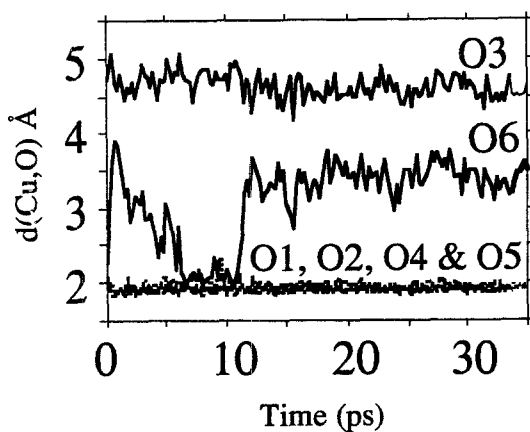


Fig. 10. The $\text{Cu}^{2+}/2$ conformer of the **Calix6**- Cu^{2+} complex in water. $\text{Cu}^{2+} \dots \text{O}_p$ distances as a function of time.

TABLE VII. **Calix6**- Cu^{2+} in water. Energy component analysis based on the interaction of 4 groups: the calixarene, the Cu^{2+} ion, the water molecules at less than 5 Å from U, and the other water molecules. Average energies and fluctuations from the MD trajectories, in kJ mol^{-1} .

		Calix6	Water shell at 5 Å from Cu^{2+}	Other water molecules
Cu^{2+}	a	-5583 ± 4	273 ± 5	818 ± 6
	b	-5585 ± 3	156 ± 3	968 ± 4
Calix6	a	4943 ± 5	-580 ± 8	-3674 ± 14
	b	4840 ± 5	-735 ± 4	-4040 ± 14
Water shell at 5 Å from Cu^{2+}	a		5 ± 1	-103 ± 3
	b		77 ± 4	-240 ± 3
Other water molecules	a			-31862 ± 28
	b			-37420 ± 400

^a $\text{Cu}^{2+}/1$ conformer.

^b $\text{Cu}^{2+}/2$ conformer.

the dehydration of the carbon upon complexation is more extensive for UO_2^{2+} than for Cu^{2+} , which remains directly coordinated to water.

4. Conclusions

We have presented a theoretical investigation of the **Calix6** uranophile in water, and on its complexes with UO_2^{2+} and a spherical M^{2+} cation. This was referred to as Cu^{2+} for simplicity, but other cations such as Ca^{2+} , with a similar size, would have similar behavior. MD simulations on **Calix6** and its complexes with Cu^{2+} and UO_2^{2+} have been performed first in the gas phase, then in water, assuming that the cation is coordinated to the phenolic oxygens of the ligand. **Calix6** is found to adopt different geometries in its free and complexed states, in the gas phase and in water. The conformation simulated for the calixarene free **Calix6** or within its complexes with UO_2^{2+} and Cu^{2+} also differs from the forms of the free calix[6]arene in the solid state, in its neutral state [4, 32]. In aqueous solution, the hydration pattern in the hydrophilic region of the complex depends markedly on the shape (linear/spherical) of the cationic guest. In the UO_2^{2+} and the $\text{Cu}^{2+}/1$ complexes, the cation is well encapsulated and not coordinated directly to solvent molecules. In the most stable $\text{Cu}^{2+}/2$ complex, the calixarene has rearranged to allow direct water coordination to the cation.

Several theoretical questions remain to be investigated further, concerning particularly the treatment of electrostatic interactions (polarization effects [59], long range electrostatics and cut-off [60]) and the conformational sampling [61]. The stereochemical requirements of binding UO_2^{2+} in a pseudoplanar mode, as compared to the tetrahedral arrangement surrounding Cu^{2+} , was not explicitly incorporated in our force field calculations, and is expected to disfavour Cu^{2+} in these calixarene complexes. Our theoretical study strongly suggests that the selective binding of UO_2^{2+} relative to spherical cations depends not only on the nature, size and precise arrangement of the binding sites of the ionophore, but also on *solvent effects*. Schematically, once the U atom is properly surrounded in the equatorial plane by the ligands, it does not need first-shell coordination with water, as do the complexed spherical cations. The release of water upon complexation of UO_2^{2+} by calixarenes may therefore be more important than for other divalent ions [62]. Given the difference in solvation of UO_2^{2+} compared to spherical cation complexes, it can be speculated that a counterion effect, if any, may be also very different for these cationic species. Thermodynamic measurements on the enthalpy and entropy components of the free energy of binding should provide interesting insight into the binding selectivity for uranyl [62].

From the modeling side, complexes involving the upper rim sulfonato groups for binding uranyl cannot be completely ruled out, since the derivative of calix[6]arene, with six phosphonomethyl groups at the upper rim and six methoxy groups at the lower rim, also binds UO_2^{2+} strongly in water, presumably via the negatively charged upper rim groups [2]. Such complexes cannot be compared accurately enough with force field representations of the potential energy. It is at present a very challenging task, to account for the pH and conformation-dependent competition of phenolic and sulfonato binding sites to the cationic guest.

Acknowledgements

The authors are very grateful to the CEA for financial support, and to Etienne Engler for computational assistance. M. Silvestri is acknowledged for linguistic assistance.

References

1. I. Tabushi and Y. Kokube: *Isr. J. Chem.*, 217 (1985).
2. T. Nagasaki, T. Arimura and S. Shinkai: *Bull. Chem. Soc. Jpn.* **64**, 2575 (1991).
3. S. Shinkai, H. Koreishi, K. Ueda, T. Arimura and O. Manabe: *J. Am. Chem. Soc.* **109**, 6371 (1987).
4. J.L. Atwood, D.L. Clark, R.K. Juneja, G.W. Orr, K.D. Robinson and R.L. Vincent: *J. Am. Chem. Soc.* **114**, 7558 (1992).
5. T. Nagasaki, K. Kawano, K. Araki and S. Shinkai: *J. Chem. Soc. Perkin Trans. 2*, 1325 (1991).
6. C.D. Gutsche: *Calixarenes*, J.F. Stoddart (Ed.), U.K.; Royal Society of Chemistry (1989). J.L. Atwood: 'Cation Complexation by Calixarenes', in *Cation Binding by Macrocycles*, Y. Inoue and G. Gokel (Eds.), M. Dekker, New York, p. 581 (1991).
7. J.-P. Scharff, M. Mahjoubi and R. Perrin: *New J. Chem.* **15**, 883 (1991). See also studies on calix[4]arenes: I. Yoshida, N. Yamamoto, F. Sagara, D. Ishii, K. Ueno and S. Shinkai: *Bull. Chem. Soc. Jpn.* **65**, 1012 (1992). L.C. Groenen, E. Steinwender, B.T.G. Lutz, J.H. van der Maas and D.N. Reinhoudt: *J. Chem. Soc. Perkin Trans. 2*, 1893 (1992). S. Shinkai, K. Araki, P.D.J. Grootenhuys and D.N. Reinhoudt: *J. Chem. Soc. Perkin Trans. 2*, 1883 (1991).
8. M. Dobler: *Ionophores and Their Structures*, Wiley Interscience, New York, 1981.
9. R.M. Izatt, K. Pawlak, J.S. Bradshaw and R.L. Bruening: *Chem. Rev.* **91**, 1721 (1991).
10. Y. Inoue and G. Gokel: in *Complexation of Cationic Species by Crown Ethers*, M. Dekker, New York and Basel (1992).
11. T.S. Franczyk, K.R. Czerwinski and K.N. Raymond: *J. Am. Chem. Soc.* **114**, 8138 (1992).
12. Y. Marcus: *Ion Solvation*, J. Wiley, Chichester (1985).
13. R.D. Rogers, A.H. Bond and W.H. Hipple: *J. Crystallogr. Spectrosc. Res.* **22**, 365 (1992).
14. A. Navaza, F. Villain and P. Charpin: *Polyhedron* **3**, 143 (1984).
15. P.G. Eller and R.A. Penneman: *Inorg. Chem.* **15**, 2439 (1976).
16. J.M. Lehn: *Struct. Bonding* **16**, 60 (1973); *Angew. Chem. Int. Ed. Engl.* **27**, 89 (1988).
17. W.L. Jorgensen, J. Chandrasekhar and J.D. Madura: *J. Chem. Phys.* **79**, 926 (1983).
18. P. Guilbaud and G. Wipff: *J. Phys. Chem.* **97**, 5685 (1993).
19. S.P. Best, R.J.H. Clark and R.P. Cooney: *Inorg. Chim. Acta* **145**, 141 (1988).
20. M. Brighli, J. Lagrange and P. Lagrange: *Polyhedron* **3**, 469 (1984).
21. A. Dejean, P. Charpin, G. Folcher, P. Rigny, A. Navaza and G. Tsoucaris: *Polyhedron* **6**, 189 (1987).
22. A. Fratiello, V. Kubo and R.E. Schuster: *Inorg. Chem.* **10**, 744 (1971).
23. P. Fux, J. Lagrange and P. Lagrange: *J. Chim. Phys.* **81**, 321 (1984).
24. R. Graziani, G. Bombieri and E. Forsellini: *J. Chem. Soc. Chem. Commun.*, 2059 (1972).
25. J. Lagrange, P. Lagrange, J.P. Metabanzoulou and P. Fux: *Polyhedron* **8**, 2251 (1989).
26. R.D. Rogers, A.H. Bond, W.G. Hipple, A.N. Rollins and R.F. Henry: *Inorg. Chem.* **30**, 2671 (1991).
27. L. Rodehüser, P.R. Rubini, K. Bokolo and J.-J. Delpuech: *Inorg. Chem.* **21**, 1061 (1982).
28. R.D. Rogers, M.M. Benning, R.D. Russel, D. Etzenhouser and A.N. Rollins: *J. Chem. Soc. Chem. Commun.*, 1586 (1989).
29. R.D. Rollins and M.M. Benning: *J. Incl. Phenom.* **11**, 121 (1991).
30. D.M. Rudkevich, W.P.R.V. Stauthamer, W. Verboom, J.F.J. Engbersen, S. Harkema and D.N. Reinhoudt: *J. Am. Chem. Soc.* **114**, 9671 (1992).
31. T.J. Hall, C.J. Mertz, S.M. Bachrach, W.G. Hipple and R.D. Rogers: *J. Crystallogr. Spectrosc. Res.* **19**, 499 (1989).
32. G.D. Andreotti and F. Uguzzoli: *Gaz. Chim. Ital.* **119**, 47 (1989).

33. P. Auffinger and G. Wipff: *J. Am. Chem. Soc.* **113**, 5976 (1991).
34. G. Wipff: *J. Coord. Chem.* **27**, 7 (1992).
35. J.-L. Toner: *Modern Aspects of Host-Guest Chemistry: Molecular Modeling of Conformationally Restricted Hosts in 'Crown Ethers and Analogs'*, S. Patai, Wiley Interscience Publ., 77 (1989); G. Wipff: *Computational Approaches in Supramolecular Chemistry*, NATO ASI, Kluwer (1994) and references cited therein.
36. P.V. Maye and C.A. Venanzi: *J. Comput. Chem.* **12**, 994 (1991); C.A. Venanzi, P.M. Canzius, Z. Zhang and J.D. Bunce: *J. Comput. Chem.* **10**, 1938 (1989).
37. L.X. Dang and P.A. Kollman: *J. Am. Chem. Soc.* **112**, 5716 (1990); J. van Eerden, W.J. Briels, S. Harkema and D. Feil: *Chem. Phys. Lett.* **164**, 370 (1989); J. van Eerden, S. Harkema and D. Feil: *J. Phys. Chem.* **92**, 5076 (1988).
38. T.J. Marrone and K.M. Merz: *J. Am. Chem. Soc.* **114**, 7542 (1992).
39. M.H. Mazor, J.A. McCammon and T.P. Lybrand: *J. Am. Chem. Soc.* **112**, 4411 (1990).
40. G. Eisenman, O. Alvarez and J. Aqvist: *J. Incl. Phenom.* **12**, 22 (1992); J. Aqvist, O. Alvarez and G. Eisenman: *J. Phys. Chem.* **96**, 10019 (1992).
41. P.A. Kollman and K.M. Merz: *Acc. Chem. Res.* **23**, 246 (1990).
42. J. Royer, F. Bayard and C. Decoret: *J. Chim. Phys.* **87**, 1695 (1990).
43. S. Miyamoto and P.A. Kollman: *J. Am. Chem. Soc.* **114**, 3668 (1992). See also L.C. Groenen, J.A.J. Brunink, W.I.I. Bakker, S. Harkema, S.S. Wijmenga and D.N. Reinhoudt: *J. Chem. Soc. Perkin Trans. 2*, 1899 (1992).
44. P.D.J. Grootenhuys, P.A. Kollman, L.C. Groenen, D.N. Reinhoudt, G.J.V. Hummel, F. Ugozzoli and G.D. Andreotti: *J. Am. Chem. Soc.* **112**, 4165 (1990).
45. P. Guilbaud, A. Varnek and G. Wipff: *J. Am. Chem. Soc.* **115**, 8298 (1993).
46. A. Varnek and G. Wipff: *J. Phys. Chem.* **97**, 10840 (1993).
47. D.A. Pearlman, D.A. Case, J.C. Cadwell, G.L. Seibel, U.C. Singh, P. Weiner and P.A. Kollman: AMBER4, University of California, San Francisco (1991).
48. P.K. Weiner and P.A. Kollman: *J. Comput. Chem.* **2**, 287 (1981); S.J. Weiner, P.A. Kollman, D.T. Nguyen and D.A. Case: *J. Comput. Chem.* **7**, 230 (1986).
49. T.M. Fyles: 'Electrostatic Ion Binding by Synthetic Receptors', in Ref. 10, p. 203.
50. P. Guilbaud, P. Legrand and G. Wipff: unpublished results.
51. F. Ugozzoli and G.D. Andreotti: *J. Incl. Phenom.* **13**, 337 (1992).
52. E. Engler and G. Wipff: unpublished results.
53. L.C. Groenen: 'Conformational Properties of Calixarenes', Thesis, University of Twente (1992).
54. X.D. Liem and P.A. Kollman: *J. Am. Chem. Soc.* **112**, 5716 (1990); P.A. Kollman, *Chem. Rev.* **93**, 2395 (1993).
55. J. Cullinane, R.I. Gelb, T.N. Margulis and L.J. Zompa: *J. Am. Chem. Soc.* **104**, 3048 (1982).
56. E. Kauffmann, J.-M. Lehn and J.-P. Sauvage: *Helv. Chim. Acta* **59**, 1099 (1976).
57. H.J. Schneider, T. Schiestel and P. Zimmermann: *J. Am. Chem. Soc.* **114**, 7698 (1992).
58. P. Auffinger and G. Wipff: *J. Chimie Phys.* **88**, 2525 (1991); T.P. Lybrand, J.A. McCammon and G. Wipff: *Proc. Natl. Acad. Sci. USA* **83**, 833 (1986). See also W.L.J. Jorgensen: *Acc. Chem. Res.* **22**, 184 (1989) and references cited therein.
59. J. Caldwell, L.X. Dang and P.A. Kollman: *J. Am. Chem. Soc.* **112**, 9144 (1990). A.E. Howard, U.C. Singh, M. Billeter and P.A. Kollman: *J. Am. Chem. Soc.* **110**, 6884 (1988). K. Ramnarayan, B.G. Rao and U.C. Singh: *J. Chem. Phys.* **92**, 7057 (1990). A. Warshel and S.T. Russell: *Quart. Rev. Biophys.* **17**, 283 (1984).
60. C.L. Brooks III, B.M. Pettitt and M. Karplus: *J. Chem. Phys.* **83**, 5897 (1985). J.D. Madura and B.M. Pettitt: *Chem. Phys. Lett.* **150**, 105 (1988). J.B. Matthew: *Ann. Rev. Biophys. Biophys. Chem.* **14**, 387 (1985). J. Guenot and P.A. Kollman: *J. Comput. Chem.* **14**, 295 (1993). P.E. Smith and B.M. Pettitt: *J. Chem. Phys.* **95**, 8430 (1991).
61. P. Auffinger and G. Wipff: *J. Comput. Chem.* **11**, 19 (1989). T.P. Straatsma and J.A. McCammon: *J. Chem. Phys.* **91**, 3631 (1989). Y. Sun and P.A. Kollman: *J. Comput. Chem.* **12**, 33 (1992).
62. Y. Inoue and T. Hakushi: 'Thermodynamics of Cation-Macrocyle Complexation: Enthalpy-Entropy Compensation' in Ref. 10, p. 1.